Effects of the Aging Temperature on the Mechanical Properties and Microstructures of Al-5.1Zn-1.8Mg-0.4Ti wt.% Alloy Produced by Squeeze Casting

Desrilia Nursyifaulkhair, Risly Wijanarko, Irene Angela and Bondan T. Sofyan
Department of Metallurgy and Materials Engineering, Faculty of Engineering, Universitas Indonesia, Depok, Indonesia
Email: bondan@eng.ui.ac.id

***Abstract*— In this paper, the role of Ti in the precipitation strengthening of the Al-5.1Zn-1.8Mg-0.4Ti (wt.%) was studied. Al-Zn-Mg alloys (Al 7xxx series) have been widely used in industrial applications that require high-strength and low-density requisition, such as the aerospace industry. These alloys are commonly age-hardened, in which the diffusion of Zn and Mg atoms is incorporated from a supersaturated solid solution (SSSS), resulting in the formation of metastable precipitates. Ti is added to decrease the grain size, thus increasing the strength of the alloys. Fabrication of the alloy was carried out using squeeze casting, followed by homogenization at 400°C for 4 h. A subsequent solution treatment was employed at 440°C for 1 h, followed by water quenching. Aging was carried out at 90, 130, and 200°C for up to 200 h. Characterization was performed using Rockwell hardness testing, optical microscopy, and scanning electron microscopy-energy dispersive spectroscopy (SEM-EDS). The highest hardness was achieved in samples aged at 90°C. Higher aging temperatures decreased both the number and the time needed to achieve peak hardness. The addition of Ti was found to retard the strengthening effect by slowing down the kinetics of precipitation through decreasing the number of solute-vacancy complexes. The suggested major precipitation sequence is as follows: GP zones → η′ → η ($MgZn_2$).**

***Index Terms*—Aluminum alloy, titanium, precipitation, aging**

I. Introduction

High-strength low-density Al-Zn-Mg alloys (Al 7xxx series) are widely used under high-demand operating conditions (e.g., in the aerospace industry). Controlling the alloy's composition and produced morphology performed via altering the alloying element fractions and heat treatment parameters in order to obtain high-strength as-cast Al-Zn-Mg [1]. Nurcahyaningsih [2] carried out an aging treatment on an Al-10Zn-6Mg wt.% alloy at 130°C, obtaining a peak hardness of 172 HV. The aging treatment of the Al-4Zn-1.5Mg-0.9Cu wt.% alloy at 120°C that was performed by Syakura [3] showed a 93.93 HV peak hardness. Nurcahyaningsih [2] used a higher content of Zn and Mg to allow more precipitates to form, thus obtaining a higher peak hardness than that found in the experimental alloy of Syakura [3].

Al-Zn-Mg alloys are generally strengthened using the T6 heat treatment method, which consists of solution treatment, quenching, and aging sequences. Heat-treated alloys experience an increase in hardness owing to the formation of metastable precipitate phases η′ and T' [4, 5]. The precipitate formation sequence in Al-Zn-Mg alloys is generally as follows: SSSS → GP zone → η′ → η ($MgZn_2$) or SSSS → T′ → T ($Mg_3Zn_3Al_2$). Higher aging temperatures boost precipitate formation rate, but the peak hardness will not be higher than those at lower aging temperatures owing to the incoherent structure transformation of precipitates [6, 7].

The addition of a grain-refining agent, such as Ti, is a means to produce Al-Zn-Mg alloys with higher strength and hardness [8]. Well-distributed $TiAl_3$ acts as a nucleating agent that allows finer homogenous α-Al grains and more intermetallic precipitates to form [9], whereas dissolved Ti also works as a growth-retarding agent during solidification. However, $TiAl_3$ has a certain fading time, in which its efficiency as a grain-refining agent decreases [10].

Gao [8] showed that the presence of Ti during aging treatment contributes to establishing a large number of fine (Zr-Ti)Al_3 precipitates to rough η′($MgZn_2$) in Al-6Zn-2Mg-2.5Cu-0.2Zr-0.2Ti wt.% alloys, thus yielding a final aged product with improved strength. Lestari [11] showed similar strengthening from 54.29 to 64.07 HRB of ZrO_2-reinforced as-cast Al-10Zn-6Mg-3Si (wt.%) composites with up to 0.1041 wt.% Ti addition. Following solution treatment for 1 h and aging at 200°C for 1 h on the previous composites with Ti addition [11], a corresponding increase of hardness to 65.22 HRB was obtained. This limited strengthening was suggested to occur as a result of the restricted precipitation kinetics in accordance with the reaction of Ti with vacancy or solute elements. Reciprocally, an increase in hardness from 49.72 to 52.08 HRB was found with the addition of Ti in as-cast Al-10Zn-6Mg wt.% alloys due to the decrease in the Secondary Dendrite Arm Spacing (SDAS) value and

Manuscript received April 4, 2018; revised December 5, 2018.

doi: 10.18178/ijmerr.8.1.92-98

increase in the Growth Restriction Factor (GRF) number resulting from the addition of Ti [2].

The solubility limit of the GP zone in Al-5.32Zn-1.66Mg-0.041Ti wt.% during aging was estimated at 145^{o}C [12], whereas the formation of the GP zone, η′, and η ($MgZn_2$) phases was observed at 40, 180, and 460^{o}C, respectively, in another research using simultaneous thermal analysis (STA) [2]. Hence, it can be assumed that the GP zone will appear in the precipitation mechanism by aging at temperatures below 200^{o}C, while higher aging temperatures will result in η′($MgZn_2$) precipitates. Therefore, the responses of the Al-5.1Zn-1.8Mg-0.4Ti wt.% alloy during aging at different temperatures after solution treatment at 440^{o}C for 1 h were investigated in this research using compositional analysis, hardness testing, and microstructure observation.

II. Experimental Procedure

Commercial pure Al (99.76 wt.%), Zn (99.99 wt.%), and Mg (99.90 wt.%) ingots and Al-5Ti-1B master-alloy rods were used to produce the experimental Al-5.1Zn-1.8Mg-0.4Ti wt.% alloy. The ingots and rods were melted gradually in a graphite crucible at 850^{o}C, degassed with argon for 1 min, and stirred at 5,000 rpm for 2 min. The melts were poured into a 170 × 170 × 15 mm^3 preheated metal mold and squeeze-casted at 76 MPa for 10 min. The casted plate was then homogenized at 400^{o}C for 4 h. The samples were then heat treated using the T6 procedure, which included solution treatment at 440^{o}C for 1 h, water quenching, and aging at 90, 130, and 200^{o}C in a silicon oil bath for up to 200 h.

Sample characterization was performed via compositional analysis using an Ametek SPECTROMAXx optical emission spectroscope and Rockwell B hardness testing method in accordance with the ASTM E18 standard. The microstructures were observed by scanning electron microscope-energy dispersive spectroscopy (SEM-EDS) (Quanta 650) and a Zeiss Primotech optical microscope with standard metallographic preparation using a Keller etchant made of 5% HNO_3, 3% HCl, 2% HF, and balanced distilled water. The calculation of the SDAS values was performed on microstructures of as-cast samples with 50x magnification using Matscope. STA was conducted using an STA 6000 (ParkinElmer, Waltham, MA, USA) at 50-500^{o}C with 10 ^{o}C/min scanning rate to investigate the heat fluctuation, phase transformation, and material crystallinity as a function of time or temperature.

III. Results and Discussion

A. *Microstructural Evolution and Hardness of As-Cast and As-Homogenized Alloys*

Fig. 1 shows the microstructure of as-cast Al-5.1Zn-1.9Mg and Al-5.1Zn-1.8Mg-0.4Ti wt.% alloys. The Interdendritic phase in dark contrast could be observed in both alloys (red arrows). An amount of shrinkage that was caused by the different cooling rates during the solidification process (blue arrows) was also observed. Different dendrite structures can be easily observed in the figure. Without the addition of Ti, the dendritic structure of the alloy tended to be long and sharp, with an average SDAS value of 37.5 µm, as shown in Fig. 1 (a). Figure 1 (b) shows no remaining dendritic structures in the alloy, but fine round-shaped grains of 67.3 µm after adding 0.4 wt.% Ti.

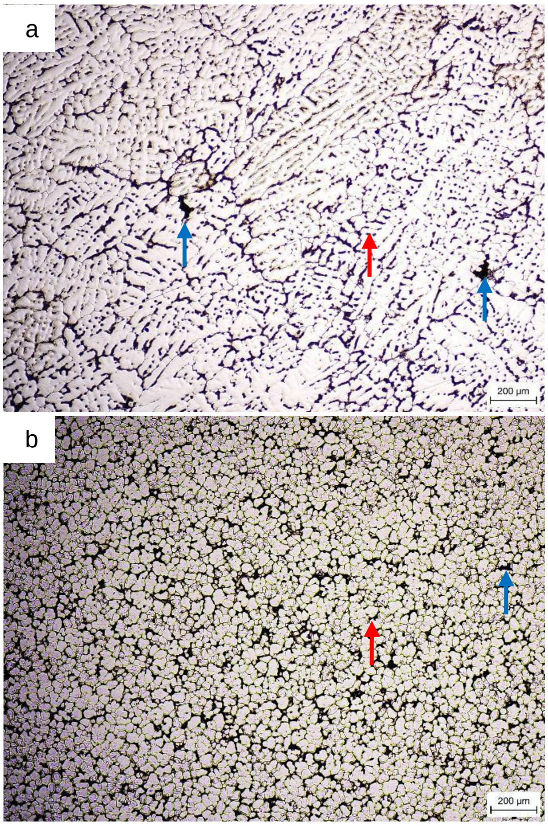

Figure 1. As-cast microstructures of (a) Al-5.1Zn-1.9Mg [13] and (b) Al-5.1Zn-1.8Mg-0.4Ti wt.% alloys.

Grain refining in the Al-5.1Zn-1.8Mg-0.4Ti alloy was achieved by GRF number (*Q*) and nucleation by $TiAl_3$. A higher GRF number leads to the formation of finer grains. The GRF numbers of alloys with and without Ti addition were 105.17 and 7.23, respectively. Thus, it is indicated that Ti promoted more grain restriction. Ti-induced nucleation occurred in the reaction between $TiAl_3$ and Al, which initiated the growth of the nuclei during solidification. The grain-refining mechanisms resulted in increased hardness by means of grain boundary strengthening. This was proven by the hardness testing results of both alloys, which were 50.3 HRB in Al-5.1Zn-1.9Mg and 54.1 HRB in Al-5.1Zn-1.8Mg-0.4Ti.

Due to the higher cooling rate in the casting process, which causes an inhomogeneity, it is necessary to eliminate or reduce serious segregation by homogenization treatment. The homogenized microstructure of the studied alloy is shown in Fig. 2. After homogenization, most of the brittle interdendritic phases started to dissolve into the α-Al matrix and then transformed the grains to equiaxed grains. Furthermore, Fig. 3 shows an X-ray mapping of the Al-5.1Zn-1.8Mg-0.4Ti wt.% alloy. It can be inferred that Mg and Zn were uniformly distributed in the α- Al matrix. In addition, Ti elements were found to segregate in grain boundaries and appear in the grains as white spots. The Ti segregation and white spots indicated the growth restriction and $TiAl_3$ that acts as a nucleant in the alloy, respectively. Moreover, the elements not detected by X-ray are shown as black spots, as can be seen in the figure. Meanwhile, due to the homogenization treatment, the hardness value of the as-homogenized alloy decreased from 54.1 to 51.93 HRB.

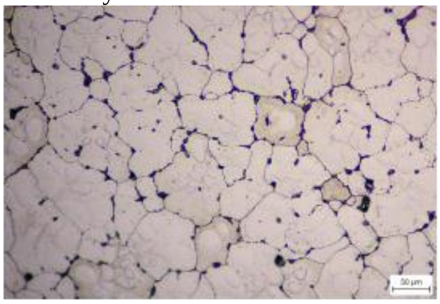

Figure 2. As-homogenized microstructure of the Al-5.1Zn-1.8Mg-0.4Ti wt.% alloy.

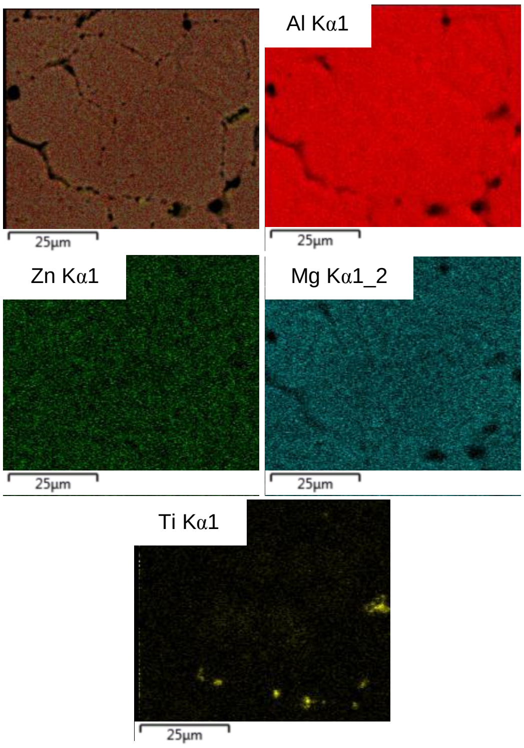

Figure 3. X-ray mapping of the as-homogenized Al-5.1Zn-1.8Mg-0.4Ti wt.% alloy.

Figure 4 shows the SEM-EDS micrographs of the Al-5.1Zn-1.8Mg-0.4Ti wt.%. The results of the EDS characterization at three positions are presented in Table 1. At Point 1, it revealed to be the α-Al matrix area with no Ti. Meanwhile, Point 2 was noticed to be the grain boundary in the interdendritic area. No Ti was observed in the grain boundaries. This is different from the X-ray mapping in Fig. 3, because SEM-EDS is a point analysis. This suggests that Ti tends to segregate at the grain boundaries in an inhomogeneous manner. Point 3 was indicated as the matrix, which contained of Ti. In accordance with the EDS results, the white spots contained 0.19 wt.% Ti, which was not detected in the darker matrix. This supports the notion that $TiAl_3$ acts as a nucleating agent.

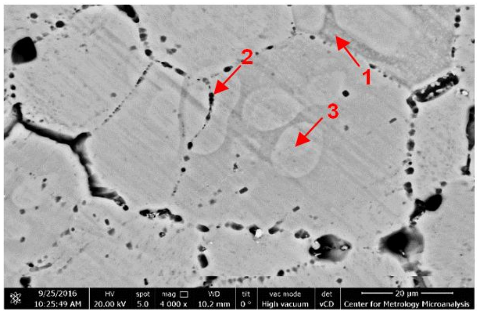

Figure 4. SEM micrograph of the as-homogenized Al-5.1Zn-1.8Mg-0.4Ti wt.% alloy.

TABLE I. EDS CHARACTERIZATION OF AL-5.1ZN-1.8MG-0.4TI WT.% ALLOY AT POSITIONS AS SHOWN IN FIG. 4.

Position	Elemental content (at.%)				Possible phase
	Al	Zn	Mg	Ti	
1	95.77	2.09	2.14	—	α-Al matrix
2	95.46	2.42	2.12	—	α-Al matrix
3	96.18	1.85	1.78	0.19	α-Al matrix

B. Aging Characteristics

1) Age hardening curve

Figure 5 illustrates the age hardening responses of the studied alloy with and without Ti addition. As can be seen, the hardness value of the Al-5.1Zn-1.8Mg-0.4Ti wt.% alloy decreased from 54.1 to 51.9 HRB after homogenization due to the grain size transformation to equiaxed grains, which increased the alloy's ductility. After solution treated at 440 ℃ for 1 h and quenched, the hardness value significantly decreased to 24.54 HRB. This phenomenon might occur due to the dissolution of alloy elements, which are Zn and Mg, into the α-Al matrix. In addition, the quenching process trapped and generated vacancies in the lattice structure. This resulted in a relatively soft and weak SSSS matrix. However, the existing vacancies can aid in precipitation during subsequent aging.

After quenching, aging treatment was performed and then the hardness value gradually increased. When aging was carried out at 90 ℃, the hardness value increased to 28.48 HRB in the first 5 min and then significantly increased to 74.4 HRB after 200 h of aging. Meanwhile, a different response was observed at the aging temperature of 130 ℃. Incubation time occurred in the first aging time of 5 min to 1 h, in which GP zones started to be arranged. The hardness value at this condition was 29.6–32.36 HRB. Furthermore, hardness reached its maximum value, 63.78 HRB, at 48 h owing to the transformation of GP zones to semicoherent precipitates. However, it then decreased when aging time reached 200 h. This indicates the change of precipitate interface from semicoherent to incoherent, which eliminates stresses in the lattices. The hardness value of the Al-5.1Zn-1.8Mg-0.4Ti wt.% alloy was 28.74 HRB after aging at 200 ℃ for 5 min. Peak hardness was then achieved at 40.58 HRB at an aging time of 4 h, which indicated the formation of semicoherent precipitates. After aging for 96 h, the hardness value decreased to 29.9 HRB, which signifies incoherent precipitate formation.

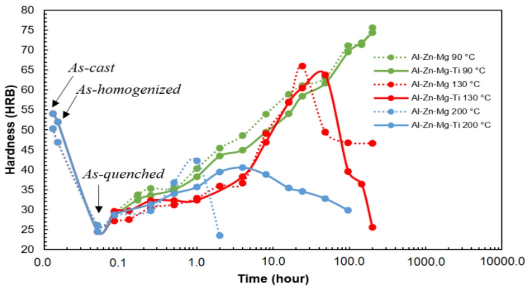

Figure 5. Aging characteristics of the Al-5.1Zn-1.8Mg-0.4Ti wt.% alloy at a temperature of 90, 130, and 200 ℃.

Meanwhile, alloys without the addition of Ti showed a lower hardness under the as-cast (50.3 HRB) and the as-homogenized (46.88 HRB) conditions. Hardness also decreased after quenching to 26.1 HRB due to the diffusion of second phases into the matrix. When aging was performed at 90 ℃, the hardness value increased to 29.24 HRB in the first 5 min and continued to increase until peak hardness, 75.62 HRB, at 200 h. A similar tendency with Ti-containing alloys was seen at the temperature of 130 ℃. In the first 5 min, the hardness value increased to 27.2–30.46 HRB to arrange the GP zones, which obviously showed a lower hardness value than that with the addition of Ti. However, it then decreased to a peak hardness value of 65.94 HRB, exceeding that of Ti-containing alloys, and decreased to 46.62 HRB. At 200 ℃, the hardness value of the alloy without Ti addition increased to 22.6 HRB in the first 5 min and reached its peak value of 42.3 HRB at 1 h of aging. The hardness value significantly decreased to 28.74 HRB at 2 h. In conclusion, alloys without Ti addition have higher hardness values than those with Ti addition. This is due to the existence of Ti that restricts the formation of solute-vacancy complexes, which would be the place for precipitation to occur.

As is well known, higher aging temperatures increase the aging kinetics but decrease the precipitate nucleation. Therefore, fewer but larger precipitates formed, leading to lower peak hardness that was achieved in a shorter time. According to Fig. 5, it can be observed that GP zones formed during the initial precipitation when aging at 90 ℃ and 130°C. Meanwhile, η′ ($MgZn_2$) immediately formed at the aging temperature of 200 ℃. Thus, an incoherent precipitate could be easily formed, which led to a rapid decrease in hardness.

The microstructures of the Al-5.1Zn-1.8Mg-0.4Ti wt.% alloy aged at 90 ℃ for 15 min and 200 h are shown in Figs. 6(a) and 6(b). It can be seen that the interdendritic phase, which remains to appear in dark contrast did not completely diffuse during solution treatment. A microstructural change was observed from the under-aged to the over-aged condition where more dark particles could be detected in the over-aged condition at 200 h. The composition of the dark particles can be detected using SEM-EDS, which is shown in Fig. 7.

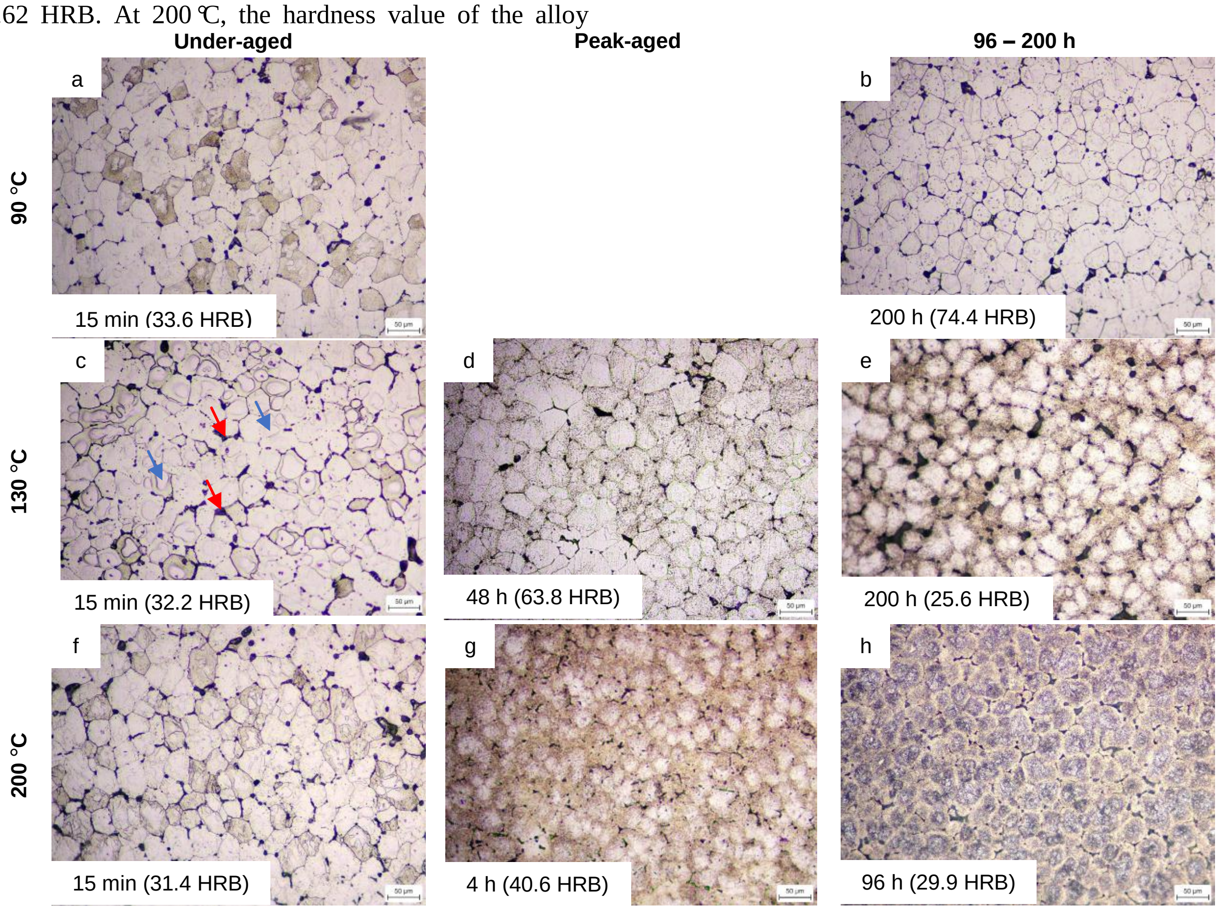

Figure 6. Microstructures of Al-5.1Zn-1.8Mg-0.4Ti wt.% alloy after aged at (a-b) 90 °C, (c-e) 130 °C, (f-h) 200 °C.

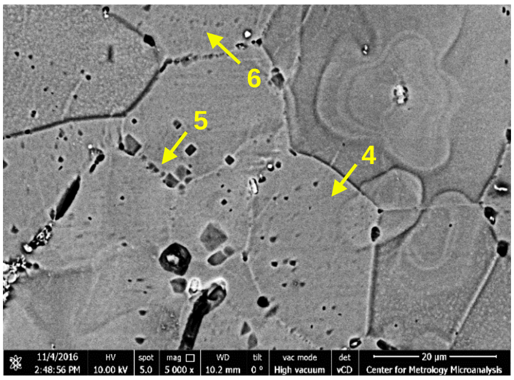

Figure 7. SEM micrograph of the as-aged Al-5.1Zn-1.8Mg-0.4Ti wt.% alloy at 90 ℃ for 200 h.

Figures 6(c)–6(e) show the microstructures of the as-aged alloy at 130°C. The interdendritic phase in dark contrast at the grain boundaries (red arrows) and white spots (blue arrows) in the grains were generally observed in the under-aged condition, which is shown in Fig. 6 (c). A considerable difference was only shown by the interdendritic phase, which was slightly thinner in comparison with the as–homogenized condition. Meanwhile, particles in the peak-aged condition seem to be adequately smaller than those in the over-aged condition. However, both conditions have similar particles, which are in dark contrast as shown in the SEM images (Fig. 8). Table 2 shows the compositions at the corresponding positions. The α-Al matrix was observed at Point 7, in which plenty of Ti elements were found and tended to be $TiAl_3$. At Points 8 and 9, the possible precipitate was η′, with a Zn/Mg ratio of 1.29 and 1.35, respectively. Ti elements at Point 9 were predicted as the solute elements that work on increasing the GRF number. Moreover, stable $MgZn_2$ was observed throughout the matrix in the over-aged condition, which is listed in Table 2.

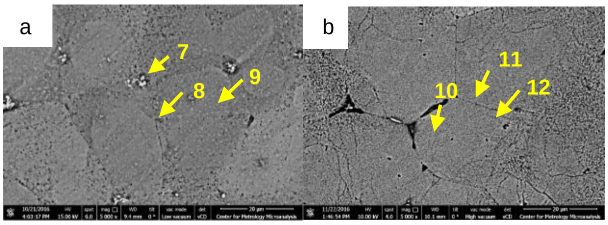

Figure 8. SEM micrographs of the as-aged Al-5.1Zn-1.8Mg-0.4Ti wt.% alloy at 130 ℃ for (a) 48 h and (b) 200 h.

2) Phase transformation

From the SEM image of the as-aged Ti-containing alloy at 90 ℃ for 200 h, it is clearly seen that the alloy has thinner interdendritic area and shows dark particles that did not appear in the as-homogenized alloy and were expected to be the precipitates. The precipitates that may appear are η ($MgZn_2$) and T ($Mg_3Zn_3Al_2$) [14]. However, the T-phase only forms if the Mg content is higher than that of Zn. Therefore, only the η-phase could be observed in the alloy. Meanwhile, no Ti elements were detected due to the maximum solubility of Ti in aluminum is only 0.15 wt.%. Thus, this indicates that not all Ti elements dissolved into the matrix.

After aging at 200 ℃, it can be seen that the microstructure at the under-aged condition is quite similar to the as-homogenized condition, as shown in Fig. 6(f). From Figs. 6(g) and 6(h), plenty of η′ phases were indicated as dark particles in the peak-aged condition, which resulted in the maximum hardness value. As presented in Table 2 (Point 13, 14, and 15), the matrix with dark particles had a Zn/Mg ratio of 1.18. Meanwhile, it was observed that the blue contrast in Fig. 6(h) seemed to indicate Ti-containing particles in the matrix in the over-aged condition, as shown in Fig. 9(b). In the over-aged condition, η-phase was tended to form and solute Ti elements were also detected. The Ti content at Points 17 and 18 was observed to be 0.68 and 0.56 wt.%, respectively. Therefore, it can be indicated that the grain refining by the Ti elements in this condition was due to the increasing number of GRF.

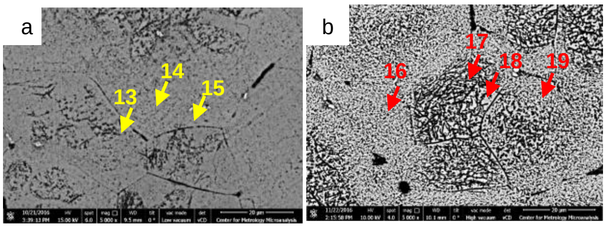

Figure 9. SEM micrographs of the as-aged Al-5.1Zn-1.8Mg-0.4Ti wt.% alloy at 200 ℃ for (a) 4 h and (b) 96 h.

TABLE II. EDS CHARACTERIZATION OF THE AL-5.1ZN-1.8MG-0.4TI WT.% ALLOY AT POSITIONS AS SHOWN IN FIGS. 7, 8, AND 9.

Position	**Elemental content (at.%)**				**Possible phase**
	Al	**Zn**	**Mg**	**Ti**	
4	95.29	2.65	1.80	—	α-Al, $MgZn_2$
5	94.91	2.89	2.20	—	α-Al, $MgZn_2$
6	95.05	2.19	2.76	—	α-Al, $MgZn_2$
7	90.95	2.15	2.89	4.01	α-Al, $TiAl_3$
8	96.12	2.23	1.65	—	α-Al, $MgZn_2$
9	95.52	2.23	1.74	0.51	α-Al, $MgZn_2$
10	94.83	2.90	2.27	—	α-Al, $MgZn_2$
11	95.07	2.73	2.20	—	α-Al, $MgZn_2$
12	95.36	2.63	2.01	—	α-Al, $MgZn_2$
13	95.45	2.46	2.09	—	α-Al, $MgZn_2$
14	95.56	2.4	2.04	—	α-Al, $MgZn_2$
15	95.7	2.33	1.97	—	α-Al, $MgZn_2$
16	97.73	1.1	1.17	—	α-Al, $MgZn_2$
17	97.53	0.84	0.95	0.68	α-Al matrix
18	97.57	0.75	1.17	0.56	α-Al matrix
19	97.7	1.06	1.24	—	α-Al, $MgZn_2$

3) Effect of Ti in aging treatment

Figure 10 shows a comparison of the aging responses on Al-5.1Zn-1.9Mg wt.% and Al-5.1Zn-1.8Mg-0.4Ti wt.% alloys after aging at 90, 130, and 200°C. The peak-aged hardness of both alloys was observed in the as-aged condition at 130°C and 200°C, whereas the as-aged hardness at the temperature of 90°C was investigated after aging for 200 h. As shown in Fig. 10, the hardness value of the Al-5.1Zn-1.8Mg-0.4Ti wt.% alloy is generally higher than that of Al-5.1Zn-1.9Mg wt.% alloy before aging. This is due to the grain refining of Ti elements, which resulted in grain boundary strengthening.

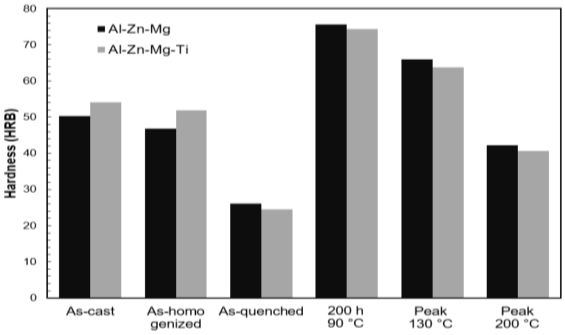

Figure 10. Hardness differences between the Al-5.1Zn-1.9Mg and the Al-5.1Zn-1.8Mg-0.4Ti wt.% alloys.

The hardness of the Ti-containing alloy increased along with the increasing aging time at the temperature of 90 ℃. However, the alloy hardness attained after aging was adequately lower (74.4 HRB) than that of the alloy without Ti addition (75.65 HRB). This indicated that the GP zone formed first, delaying the formation of η′-phase. The hardness tendency was similar to the as-aged condition at 130 ℃, which was achieved by alloy with and without Ti addition for 48 h and 24 h, respectively. Then, both alloys further showed decreasing hardness up to 200 h due to the formation of incoherent η precipitates in the matrix. Meanwhile, at the aging temperature of 200 ℃, alloys with and without Ti addition reached their peak hardness at 4 h and 1 h of aging, respectively. Thus, it can be inferred that the Al-5.1Zn-1.9Mg wt.% alloy has a higher hardness value than that of the Al-5.1Zn-1.8Mg-0.4Ti wt.% alloy after aging treatment. It also can be observed that peak hardness was achieved in a shorter time in the alloy without Ti addition. This was due to the reduction or restriction of solute-vacancy complexes formation, making it hard to form precipitates [11]. This finding is in accordance with those of Nurcahyaningsih [2], which showed a peak hardness decrease when 0–0.25 wt.% Ti was added to the Al-10Zn-6Mg wt.% alloy.

C. Phase Transformation with STA

Figure 11 shows the STA heat flow curve and its derivative of the Al-5.1Zn-1.8Mg-0.4Ti wt.% alloy. As is well known, the precipitate that would form in the Al 7xxx alloy with a Zn content higher than Mg is η ($MgZn_2$) [15]. Thus, it can be predicted that $MgZn_2$ might have precipitated in the studied alloy. In addition, it is necessary to understand the influence of Ti addition on precipitation. The heat flow curve and its derivative of Al-5.1Zn-1.9Mg wt.% alloy has been shown in Fig. 12.

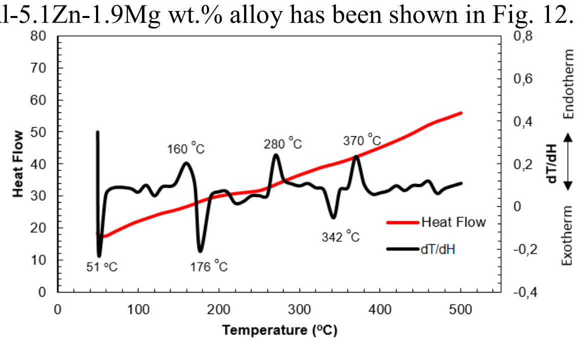

Figure 11. Heat flow curve and its derivative of the Al-5.1Zn-1.8Mg-0.4Ti wt.% alloy.

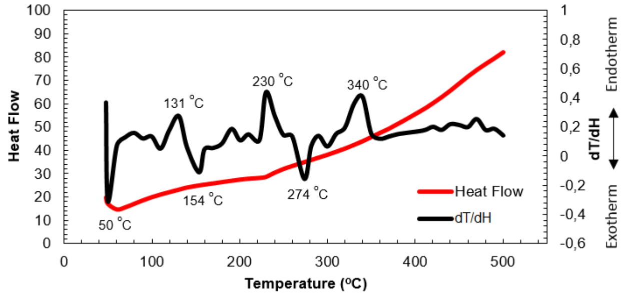

Figure 12. Heat flow curve and its derivative of the Al-5.1Zn-1.9Mg wt.% alloy.

Table III shows the formation and diffusion of the GP zone, η′-phase, and η-phase of the Al-5.1Zn-1.8Mg-0.4Ti wt.% alloy at their corresponding temperatures. It can be easily seen that the precipitate formation and diffusion of the alloy without Ti addition occur at a lower temperature compared with the alloy with Ti addition. According to Khrisna, et al. [14], the intervals of the GP zone, η′-phase, and η-phase formation are at 20–120°C, 120–250°C, and 150–300°C, respectively. Meanwhile, slightly higher diffusion temperature intervals were observed in the studied alloy, which are at 50–150°C, 200–250°C, and 300–350°C for the GP zone, η′-phase, and η-phase, respectively.

TABLE III. THE FORMATION AND DIFFUSION TEMPERATURES OF THE AL-5.1ZN-1.9MG AND AL-5.1ZN-1.8MG-0.4TI WT.% ALLOYS.

Reaction	Temperature (°C)		
	GP zone	η′	η
Al-5.1Zn-1.9Mg wt.% *			
Formation	50	154	274
Diffusion	131	230	340
Al-5.1Zn-1.8Mg-0.4Ti wt.% **			
Formation	51	176	342
Diffusion	160	280	370

*Solution-treated at 420°C.

**Solution-treated at 440°C.

Mostly, precipitate formation and diffusion of the Al-5.1Zn-1.8Mg-0.4Ti wt.% and Al-5.1Zn-1.9Mg wt.% alloys occur in those intervals. A slight difference occurred was due to the elemental composition in both alloys. As is well known, the existence Ti restricts precipitation due to the interaction between Ti and solute-vacancy complexes, which become the place to form precipitates.

IV. CONCLUSIONS

The following conclusions are drawn from the study:

(1) The addition of ~0.4 wt.% Ti to Al-5.1Zn-1.8Mg alloys increases the as-cast and as-homogenized hardness from 50.3 to 54.1 HRB and from 46.8 to 51.9 HRB, respectively. The final hardness of alloys with and without the addition of Ti decreased after solution treatment and quenching to 24.5 and 26.1 HRB, respectively.

(2) The as-cast Al-5.1Zn-1.9Mg wt.% alloy showed a dendritic microstructure with an SDAS value of 37.5 µm. The presence of 0.4 wt.% Ti in the corresponding

alloy allowed a finer and rounder grain of 67.3 μm to form.

(3) Aging on Al-5.1Zn-1.8Mg-0.4Ti wt.% at 90, 130, and 200°C resulted in peak hardness values of 74.40, 63.78, and 40.60 HRB after treatment for 200, 48, and 4 h, respectively.

(4) Higher aging temperatures will result in lower peak hardness values and will shorten the amount of time needed to achieve peak hardness.

(5) STA analysis on Al-5.1Zn-1.9Mg wt.% alloys showed that the GP zone, η′-phase, and η-phase were formed at 50, 154, and 274°C and later dissolved at 131, 230, and 340°C, respectively, whereas in Al-5.1Zn-1.8Mg-0.4Ti wt.% alloys, these phases are formed at 51, 176, and 342°C and dissolved at 160, 280, and 370°C, respectively.

Acknowledgements

This work was supported by the Directorate of Research and Community Services, Universitas Indonesia through Hibah PITTA UI 2017.

References

[1] V. V. Zakharov, T. D. Rostova, "Alloying of copper-containing aluminum alloys by scandium," *Metalloved. Term. Obrab. Met.*, vol. 2, pp. 23-27, 1995.
[2] D. A. Nurcahyaningsih, R. Wijanarko, I. Angela, B. T. Sofyan, *Matec Web of Conf.*, 186, 02009 (2018).
[3] A. Syakura, B. T. Sofyan, "Vacuum Casting Process and Analysis of Microstructure Evolution of Al-Zn-Mg-Cu Alloys with Variation in Composition during Ageing at 120 and 190 °C" (Undergrad. Thesis, Universitas Indonesia, 2011).
[4] V. I. Elagin, "History, Advantages, and Problems of Alloying of Aluminum Alloys by Transition Metals," Tekhnologiya Legkikh Splavov, **3**, 6-28 (2004).
[5] O. E. Osintev, S. L. Nikitin, "High strength corrosion-resistant cast aluminium alloys of the Al-Mg system with a high silicon content," Moscow Ins. of Aviation Tech. (2008).
[6] W. Callister, D. G. Rethwisch, *Materials Science and Engineering: An Introduction – 8th Ed.*, Hoboken, John Wiley and Sons Inc., 2009.
[7] C. A. Grove, G. Judd, Met. Trans., 4, 4, 1023-1027 (1973).
[8] T.Gao, Y. Zhang, X. Liu, Mat. Sci. & Eng. A, 598, 293-298 (2014).
[9] M. Alipour, S. Mirjavadi, M. K. Besharati Givi, H. Razmi, M. Emamy, J. Rassizadehghani, *Iranian J. Mat. Sci. & Eng*., vol. 9, no. 4, pp. 8-16 (2012).
[10] G. K. Sigworth, T. A. Kuhn, J. Metal Cast, **2**, 1, 1-12 (2007).
[11] P. I. Lestari, "Effect of Ti-B Addition on Characteristic of ZrO_2 Reinforced Al-10Zn-6Mg-3Si Composite Produced by Squeeze Casting" (Undergrad. Thesis, Universitas Indonesia, 2015).
[12] S. K. Maloney, K. Hono, I. J. Polmear, S. P. Ringer, Sripta Mater., 41, 10, pp. 1031-1038, 1999.
[13] D. P. Putra, B. T. Sofyan, IOP: Mat. Sci. and Eng., 432, 012064 (2018).
[14] K. G. Krishna, K. Sivaprasad, K. Venkateswarlu, K. C. H. Kumar, *J. Mat. Sci. Eng*., vol. 535, pp. 129-135, 2012.
[15] D. Mackenzie, Scott & Totten, E. George, *Analytical Characterization of Aluminium, Steel, and Superalloys* (Boca Raton, CRC Press, 2005).

Desrilia Nursyifaulkhair (ndesrilia@gmail.com) obtained her B.E. degree in metallurgy and materials engineering from Universitas Indonesia in 2017. Her area of scientific interest is light materials and structure.

Risly Wijanarko (rislyw@gmail.com) is currently pursuing her B.E degree in metallurgy and materials engineering at Universitas Indonesia and is expected to graduate in 2018. Her area of research interest is light materials and structure. She is currently studying the effect of solution treatment temperature on aluminium alloys.

Irene Angela (ireneangela17@gmail.com) is currently pursuing her B.E degree in metallurgy and materials engineering at Universitas Indonesia and is expected to graduate in 2018. Her area of research interest is light materials and structure. She is currently studying the effect of cold rolling and annealing temperature on brass alloys.

Bondan T. Sofyan is a Professor of Metallurgy and Materials Engineering at Universitas Indonesia. She obtained her B.E. degree from the Department of Metallurgy Engineering Universitas Indonesia, and then received her M.S. degree from the same university in 1995. She obtained her Ph.D. degree from Monash University, Australia, in 2003. Her area of research interest is light materials and structure, heat treatment, and nanotechnology.

